Journal of Fluorine Chemistry 129 (2008) 598–606

Contents lists available at ScienceDirect

Journal of Fluorine Chemistry

journal homepage: www.elsevier.com/locate/fluor

Crystalline aluminium hydroxy fluorides—Suitable reference compounds for ^{19}F chemical shift trend analysis of related amorphous solids

René König [a], Gudrun Scholz [a], Rainer Bertram [b], Erhard Kemnitz [a,*]

[a] Institut für Chemie; Humboldt Universität zu Berlin, Brook Taylor-Str. 2, 12489 Berlin, Germany
[b] Institut für Kristallzüchtung, Max Born-Str. 2, 12489 Berlin, Germany

ARTICLE INFO

Article history:
Received 29 February 2008
Received in revised form 24 April 2008
Accepted 25 April 2008
Available online 15 May 2008

Keywords:
Aluminium hydroxy fluorides
Amorphous materials
Chemical shift trend analysis
Sol–gel process
Solid-state NMR

ABSTRACT

On the basis of MAS NMR-data for crystalline $AlF_x(OH)_{3-x}\cdot H_2O$ samples in the pyrochlore structure, ^{19}F chemical shifts correlate with the average chemical composition of the octahedral environment, given by AlF_xO_{6-x} in these compounds.

The attribution of local structures in sol–gel derived amorphous $AlF_x(OX)_{3-x}\cdot XOH$ (X = H, R (alkyl)) compounds is of special interest as these or consecutively prepared solids exhibit remarkable features, for example, a high surface (HS) area accompanied by a high Lewis acidity.

By transferring this scale of a ^{19}F chemical shift trend analysis to such compounds a prediction of the chemical nature of the average Al coordination becomes possible.

A new synthetic approach to crystalline aluminium hydroxy fluorides involving a sol gel fluorination as the first reaction step and an aluminium alkoxide as precursor compound is presented. Varying the amount of HF leads to different F–OH-ratios in the $AlF_x(OH)_{3-x}$ compounds.

1. Introduction

Alkoxide precursor based sol–gel techniques are well established for the preparation of inorganic materials with remarkable properties. Studied areas of interests include mainly oxide or phosphate containing materials and their application for ceramics, optics or catalysis [1–5]. The extension on the preparation of fluoride based materials is a topical field of research and different approaches have been suggested, such as using metal trifluoroacetates [6–8] or fluorophosphates as fluorine source [9]. In 2003 we succeeded in modifying the sol–gel techniques for the preparation of fluoride materials using non-aqueous HF [10,11]. The method has proven to be useful for "convenient" synthesis of complex aluminium based fluorides (e.g. elpasolites or cryolites) [12], alkaline earth metal fluorides [13,14] or modified "doped" systems. The highly disordered metal fluorides obtained feature special characteristics: small particle or crystallite sizes open the application in optics [15] and ceramic fields and high surface (HS) areas combined with the possibility to influence the surface properties enable the utilisation of these materials for heterogeneous catalysis [16–18].

High surface-AlF_3 is one of the most important of these metal fluorides [19]. Its synthesis route involves two steps: (i) the sol–gel reaction of an aluminium alkoxide with non-aqueous HF, which leads to a xerogel, described as $AlF_x(OR)_{3-x}\cdot ROH$, after drying in vacuum. (ii) A post fluorination process with halofluoroalkanes (e.g. $CHClF_2$) gives HS-AlF_3, exhibiting an extremely high Lewis acidity, comparable to SbF_5 or the solid Lewis acids ACF or ABF [20]. The final HS-AlF_3 and the intermediate xerogel are both X-ray amorphous and comparative vibrational analysis studies of AlF_3-phases were made in order to understand structural features of the final HS-AlF_3 [21]. Preliminary investigations were concerned with local structural changes in the course of the sol–gel reaction followed by liquid state NMR [22] and MAS NMR studies on the wet and dry aluminium alkoxide fluoride gels [23].

Nevertheless, due to their amorphous highly disordered character, it is still a challenge to attribute local structures in the xerogels and to give a certain definite assignment of different $AlF_x(OR)_{3-x}$ species in these solids.

For this reason the aims of the present study are:

(i) To prepare well defined crystalline aluminium hydroxy fluorides with varying Al/F ratio through the sol–gel route followed by hydrolysis.
(ii) To find correlations between experimental MAS NMR-data of the hydroxy fluorides and their average composition of AlF_xO_{6-x} species, and also to develop a ^{19}F chemical shift

* Corresponding author. Fax: +49 30 2093 7277.
E-mail address: erhard.kemnitz@chemie.hu-berlin.de (E. Kemnitz).

0022-1139/$ – see front matter © 2008 Elsevier B.V. All rights reserved.
doi:10.1016/j.jfluchem.2008.04.015

trend analysis for the interpretation of the MAS NMR spectra of these compounds.

(iii) To apply and to test such correlations for amorphous xerogels $AlF_x(OX)_{3-x}{\cdot}XOH$ (X = H, R (alkyl)), if possible, concerning the prediction of the average chemical surrounding of Al (AlF_xO_{6-x}) in these compounds.

Finally, the resulting scheme should show a clear dependency of the physico-chemical property (in this case: chemical shift) on the local environment of the aluminium fluoride-system, as, for example, recently shown for other systems by Kramer (chemical shift trend analysis based on liquid state ^{195}Pt NMR) [24], Lacassagne (NMR studies of molten systems) [25], or at least as found in the common Wagner-Plots for XPS [26].

The method described here is well established for studying species in the bulk (MAS NMR) and together with XPS/XAES-studies, for example, it is suited for the characterisation of amorphous solids as they were used in the past several times for similar purposes [27].

1.1. $AlF_x(OH)_{3-x}$ and $AlF_x(OR)_{3-x}$—a preliminary comparison

Due to special characteristics of the crystal structure, basic aluminium fluorides were at the centre of attention a couple of times. The crystal structure of the pyrochlore phases was first discussed by Scott in 1948 [28] and later reinvestigated by Fourquet in 1988 [29] observing the protonic conductivity of these phases. Other studies involved the thermal behaviour [30], catalytic properties [31], the reactivity [32] or were comparative works about structural features in connection with acidic properties of $MF_x(OH)_{3-x}$ (M = Al^{3+}, Cr^{3+}, Fe^{3+}) in HTB-structure [33,34]. Mineralogical aspects and relationships to ralstonite were discussed by Rosenberg [35] and Desborough [36]. Additionally, some early Russian publications exist, describing different physico-chemical properties of $AlF_x(OH)_{3-x}$ as solid and in solution; among others, e.g. [37,38]. The first NMR parameters for $AlF_x(OH)_{3-x}$ were published in 1977 by Kirakosyan et al. [39]. However, no high resolution MAS NMR spectra concerning all involved nuclei ^{27}Al, ^{19}F and ^{1}H were reported for a series of solid $AlF_x(OH)_{3-x}$ phases in pyrochlore structure until now. Very recently, Dambournet published some work concerning the characterisation of related $AlF_x(OH)_{3-x}$ compounds by solid-state NMR [40,41].

Fig. 1 shows the unit cell of the crystalline hydroxy fluorides, a structural model for the aluminium alkoxide fluorides was recently published [23]. Aluminium hydroxy fluorides ($AlF_x(OH)_{3-x}$) in pyrochlore structure crystallise in the cubic space group $Fd\bar{3}m$ as described in [28,29]. The unit cell is built by 16 formula units with the aluminium atoms being centred in corner shared $AlF_x(OH)_{6-x}$-octahedrons. These form a network of channels, and other molecules (at ambient conditions mainly water) may be incorporated into the structure [28–30]. Additionally for pyrochlore-$AlF_x(OH)_{3-x}$, the fluorine amount x may vary from 1 to 2.5 [28,30,35], whereas $x = 3$ would correspond to η-AlF_3 [42]. The cell parameters vary with the fluorine content x and with the amount of incorporated water z of the hydroxy fluorides $AlF_x(OH)_{3-x}{\cdot}zH_2O$ ($z \approx 0.4-1$, see Fig. 1—black circles represent H_2O) [28,30,35]. Both aluminium and fluorine can be theoretically described by exactly one crystallographic position, but F and OH (located on the edges of the octahedrons) are statistically distributed as discussed in [29].

This implies for the solid hydroxy fluorides the possible existence of AlF_xO_{6-x}-octahedrons with different compositions, whereby the average AlF_xO_{6-x}-composition is reflected by the molar ratio F–OH of the hydroxy fluoride.

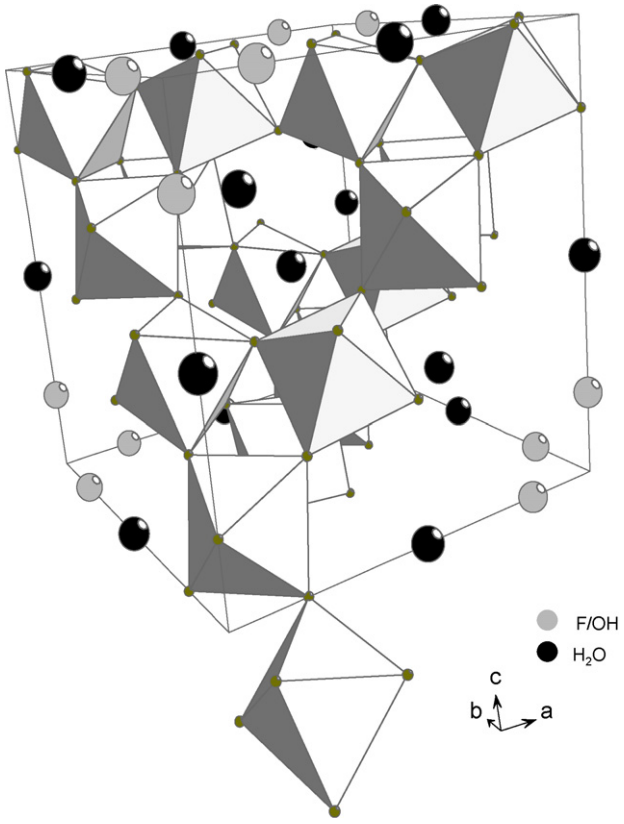

Fig. 1. Cubic unit cell (space group $Fd\bar{3}m$) of the pyrochlore-$AlF_x(OH)_{3-x}{\cdot}H_2O$. Octahedrons represent $AlF_x(OH)_{6-x}$-units, black circles water molecules, grey circles F/OH-atoms.

In opposition to the long range ordered $AlF_x(OH)_{3-x}$-phases, sol–gel derived aluminium alkoxide fluorides exhibit no long range order, as given by X-ray diffraction.

However, due to previous studies [23,43] some propositions for a structural model of the xerogel can be derived:

(i) the aluminium atoms in the bulk are mainly sixfold coordinated;
(ii) Al is surrounded by a mixed fluoride/alkoxide coordination sphere;
(iii) the $AlF_x(OR)_{6-x}$-octahedrons are mainly linked over their corners, building a network-structure, with a distribution of bond lengths and bond angles;
(iv) terminal fluorine-sites cannot be excluded, as the xerogel is sol–gel derived with a high surface area (and energy) (S_{BET} up to 400 $m^2\ g^{-1}$ and higher [19]);
(v) a definite assignment of certain $AlF_x(OR)_{6-x}$ is therefore without doubt hardly possible;
(vi) solvent (alcohol) or coordinating solvent molecules are incorporated into the structure.

So both the crystalline $AlF_x(OH)_{3-x}$ as well as the amorphous $AlF_x(OR)_{3-x}$ phases, consist of corner shared AlF_xO_{6-x}-octahedrons, which form either a regular or an irregular network. The atomic-positions for the crystalline structure are well defined. Anyway a distribution of AlF_xO_y-species is conclusive for both structures. The incorporated molecules, water on the one hand and alcohol on the other hand, interact via hydrogen bridges with the AlF_xO_y-network [23,29]. So the chemical environments for Al-atoms as well as for F-atoms of the discussed structures should be comparable. Therefore, experimental data derived from crystalline hydroxy fluoride

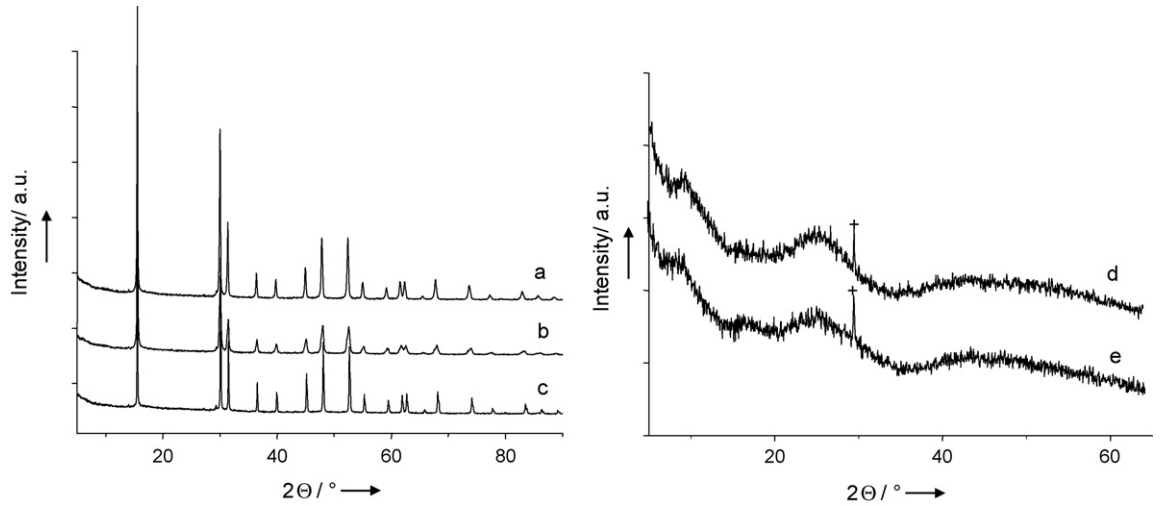

Fig. 2. X ray-powder diffractograms of the hydroxy fluorides: *a*, *b* and *c*: $AlF_x(OH)_{3-x}\cdot H_2O$ and the alkoxide fluorides *d*: $AlF_x(O^iPr)_{3-x}\cdot{}^i$PrOH and *e*: $AlF_x(OEt)_{3-x}\cdot$MeOH. +marks the reflection of the polymeric sample holder at $2\theta \approx 30^\circ$.

phases should be transferable to the interpretation of the data obtained for amorphous aluminium alkoxide fluorides.

2. Results

Fig. 2 shows a comparison of the X-ray diffractograms of the samples prepared and discussed here. Samples *a*–*c* could be identified as hydrated aluminium hydroxy fluorides with different compositions in pyrochlore structure (JCPDS-PDF-files: 04-0196 [28], resp. 41-0381 [29]), samples *d* and *e* are X-ray amorphous.

In 1966 Johnson and Siegel reported a simple path to aluminium hydroxy fluorides by thermal decomposition of $Al(O^tBu)F_2$ according to Eq. (1) [44]:

$$Al(O^tBu)F_2 \xrightarrow{200^\circ C} AlF_2(OH) + C_4H_8 \quad (1)$$

Additionally, the sol–gel route allows an easy and convenient access for the preparation of aluminium alkoxide fluorides with an adjustable F-content. These are at least intermediates for the preparation of HS-AlF_3 [19]. However, the resulting aluminium alkoxide fluorides are in the wet gelatinous state and in the dry xerogel state sensitive to moisture. The evaporation of the solvent and the hydrolysis at ambient conditions should therefore result in hydrated $AlF_x(OH)_{3-x}$ compounds in correspondence to Eq. (2):

$$Al(OR)_{3-x}F_x(\text{wet gel}) \xrightarrow{\text{air/moisture}} AlF_x(OH)_{3-x} + ROH \quad (2)$$

Three molar ratios were tested: $n(Al(O^iPr)_3):n(HF)$ 1:1; 1:2 and 1:3. The latter two led to bright white aluminium hydroxy fluorides, as confirmed by XRD (see Fig. 2a and b). The product obtained by applying the 1:1 ratio was X-ray amorphous (not included here). For the hydroxy fluoride-sample *c*, the preparation method described by Menz was followed, yielding, according to the authors, reproducible phases with the composition $AlF_{2.3}(OH)_{0.7}\cdot H_2O$ (XRD: Fig. 2c) [30], but in this study a composition $AlF_{1.9}(OH)_{1.1}\cdot H_2O$ was obtained.

On the other hand, two aluminium alkoxide fluorides were chosen as examples for this comparative study:

(a) the intermediate in the reaction to HS-AlF_3; the xerogel $AlF_x(O^iPr)_{3-x}\cdot{}^i$PrOH [19,23]; sample *d*,
(b) and a xerogel, synthesised from $Al(OEt)_3$ as starting precursor in MeOH-solution; sample *e*: $AlF_x(OEt)_{3-x}\cdot$MeOH.

However, the aluminium alkoxide fluorides are X-ray amorphous and no structural information is deducible with this method (see Fig. 2d and e and [19]).

The elemental compositions of the compounds *a*–*e* are given in Table 1. For the hydroxy fluorides *a*–*c* we found a rising fluorine content from 1.4 to 1.9 in relation to Al. The amount of water in each (determined from thermogravimetric measurements and calculated from the residual H-mass percentage) is about 1 in relation to Al.

With a closer look at the corresponding X-ray diffractograms (see Fig. 3) for *a*, *b*, and *c* it can be concluded that the observed reflections of the "sol–gel" derived $AlF_x(OH)_{3-x}$ are slightly broader in comparison to the reflections of sample *c*. Anyway, it is possible to simulate the observed powder pattern for *a* with the assumption of one phase (as done for phase *c*). The diffractogram of sample *b*

Table 1
Chemical composition of studied compounds

Mass percentages as determined by elemental analysis						Average coordination	
Sample	Al	F	C	H	Composition	AlF_xO_{6-x}	XRD
a	28.0	28	0.0	3.1	$AlF_{1.4}(OH)_{1.6}\cdot H_2O$	$AlF_{2.8}O_{3.2}$	Crystalline, one phase
b	27.2	32	1.1	3.3	$AlF_{1.7}(OH)_{1.3}\cdot H_2O$	$AlF_{3.4}O_{2.6}$	Crystalline, two phases
c	26.0	35	0.3	3.0	$AlF_{1.9}(OH)_{1.1}\cdot H_2O$	$AlF_{3.8}O_{2.2}$	Crystalline, one phase
d	n.d.	34	22.9	5.4	$AlF_x(O^iPr)_{3-x}\cdot z{}^i$PrOH		Amorphous
e	n.d.	33	11.8	4.1	$AlF_x(OEt)_{3-x}\cdot z$MeOH		Amorphous
f	n.d.	n.d.	n.d.	n.d.	$AlF_x(OH)_{3-x}\cdot zH_2O$	AlF_4O_2	Amorphous
g	n.d.	n.d.	n.d.	n.d.	$AlF_x(OH)_{3-x}\cdot zH_2O$	AlF_5O	Amorphous

n.d. not determined. The water contents for *a*–*c* were calculated from remaining H percentage, which is consistent with the water percentage calculated from thermogravimetric measurements.

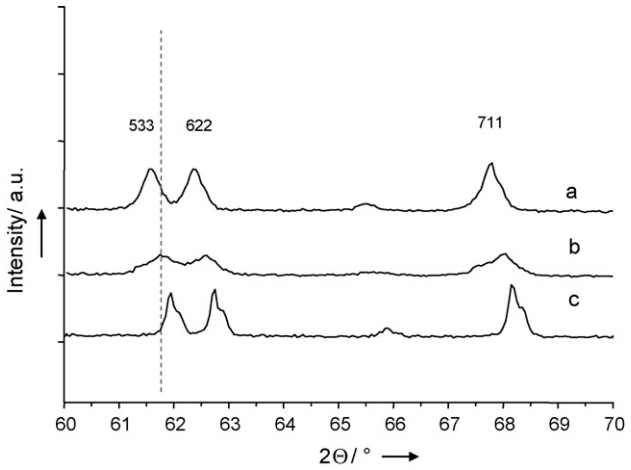

Fig. 3. X ray-diffractograms of the hydroxy fluorides: *a*, *b* and *c* and the range from $2\theta = 60^\circ$ to 70°. Additionally the appropriate *hkl*-labels are given. The shift of the reflections in dependence on the F-amount ($a < b < c$, see also Table 1) is shown. Compound *b* consists of more than one phase (see, e.g. 711-reflection).

Table 2
Cell parameters of the hydroxy fluorides as obtained by profile fitting in the space group $Fd\bar{3}m$ (Le Bail method)

Sample	Phase 1 (edge length unit cell)		Phase 2 (edge length unit cell)	
	a [Å]	Error [Å]	*a* [Å]	Error [Å]
a	9.874	0.001	–	–
b	9.882	0.001	9.835	0.001
c	–	–	9.807	0.001

could only be successfully reproduced with the superimposition of two aluminium hydroxy fluoride phases. The profile fitting with the Le Bail-method was done with the Fullprof2000 suite [45], and the corresponding graphs with residues are given in the supporting information (SI: Fig. 1). The cell parameters discovered in this way lie within the expected range as discussed by Scott [28] and are given in Table 2, the reflections get slightly shifted with a smaller unit cell (see Fig. 3).

The information deducible from the ^{1}H MAS NMR spectra for the hydroxy fluorides *a*, *b*, and *c* is nearly the same (see Fig. 4, left). The observed signals are very broad and the spectra are not very distinctive. The maximum of the main signal is found at $\delta_{cs} = 4$ ppm. Depending on the preparation method, small sharp additional peaks are possibly assignable to remaining or incorporated solvent: e.g. for *a* and *b* at $\delta_{cs} = 3.9$ and 1.1 ppm. At least a shoulder at about $\delta_{cs} = 7.5$ ppm is partially visible, which is most obvious for compound *c* (Fig. 4c). On the other hand the ^{1}H MAS NMR spectra of the xerogels *d* and *e* clearly show that a lot of solvent molecules must be incorporated in the structure: all of the signals for compound *d* at $\delta_{cs} = 1.2$, 4.4 and 7.8 ppm are attributable to ^{i}PrOH-species as already discussed in [23], and a small shoulder at $\delta_{cs} = 10.3$ ppm also indicates the existence of strongly H bridge bonded protons. For sample *e* the main signal at $\delta_{cs} = 3.4$ ppm is also assignable to incorporated solvent molecules: MeOH. For remaining ethoxide groups the peak at $\delta_{cs} = 1.2$ ppm is attributable to CH_3-groups; the signal for $-CH_2O-$ is presumably superimposed by the signal of the methanol species. A further shoulder is visible at about $\delta_{cs} = 7.5$ ppm, indicating that a hydrogen bond network ($ROH\cdots$) as found in the propoxide xerogel can be stated also for the ethoxide/methanol xerogel [23]. However, the strong relationship between the crystalline aluminium hydroxy fluorides and the amorphous aluminium alkoxide fluorides cannot be stated from ^{1}H MAS NMR.

Focussing instead on the appropriate ^{27}Al MAS NMR Fig. 5 and ^{19}F MAS NMR spectra Fig. 6, the affiliations of these two kinds of solid compounds get obvious. Nevertheless, the ^{27}Al-spectra are difficult to interpret, as the observed signals are very broad (in a range from 0 to −50 ppm) and show an asymmetric decay (upfield). The maximum of the observed signals lie between −10 and −20 ppm indicating Al-centres in an octahedral mixed fluorine/oxygen environment [46,47]. These main characteristics can be stated for all five compounds (see Fig. 5a–e). Subtle differences are at first effected by unequal distributions of AlF_xO_{6-x}-compositions of each sample, as yet reflected by elemental analysis data for *a*–*c*. In addition, a different kind of order of the involved AlF_xO_y-octahedra is present, which implies distributions of bond lengths and angles; especially for the amorphous substances. The ^{27}Al MAS spectrum of the ethoxide/methanol xerogel shows an additional peak at about 20 ppm.

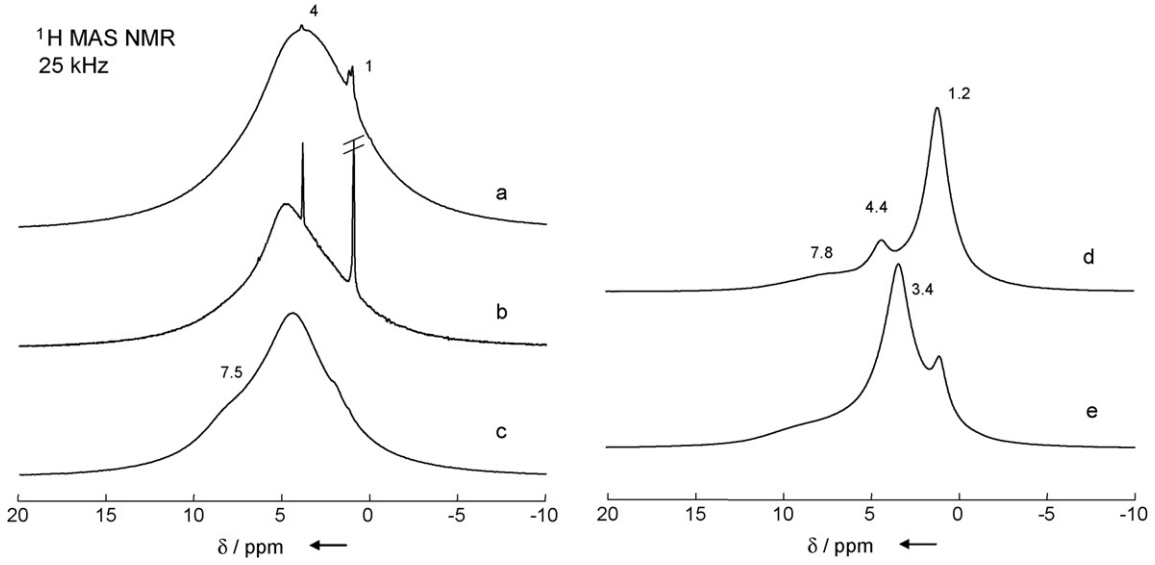

Fig. 4. ^{1}H MAS NMR spectra of the hydroxy fluorides (*a*, *b*, *c*) and the alkoxide fluorides (*d*, *e*). The spinning frequency for each is 25 kHz (number of accumulations: na): (a) $AlF_{1.4}(OH)_{1.6}\cdot H_2O$, (b) $AlF_{1.7}(OH)_{1.3}\cdot H_2O$ and (c) $AlF_{1.9}(OH)_{1.1}\cdot H_2O$; na:32, (d) $AlF_x(O^iPr)_{3-x}\cdot{}^i$PrOH; na:32, (e) $AlF_x(OEt)_{3-x}\cdot$MeOH; na: 64.

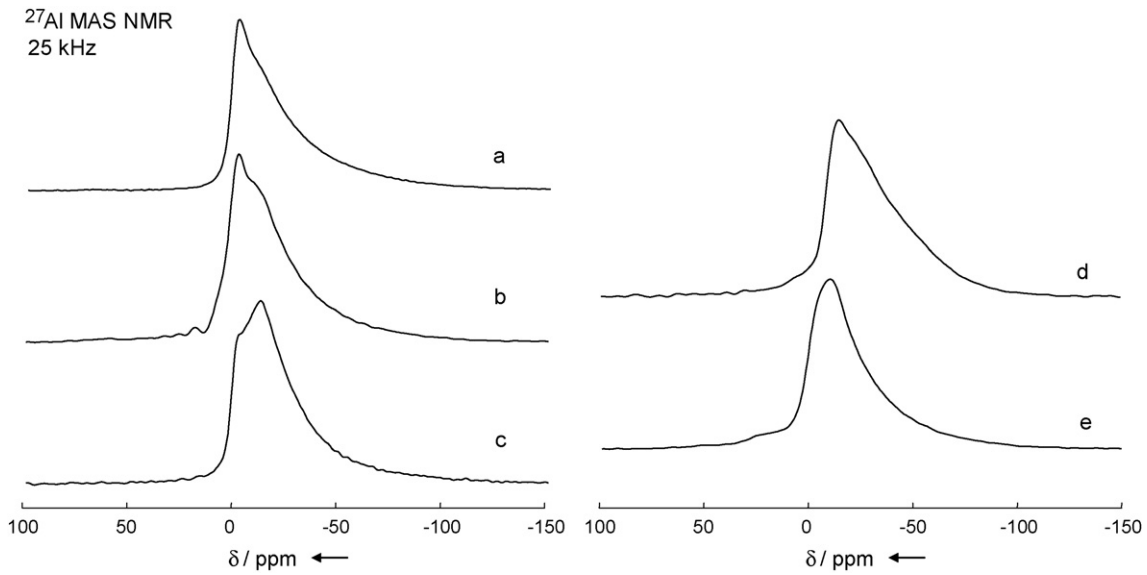

Fig. 5. ^{27}Al MAS NMR spectra of the hydroxy fluorides (*a*, *b*, *c*) and the alkoxide fluorides (*d*, *e*) at a spinning frequency of 25 kHz (number of accumulations: na): (a) $AlF_{1.4}(OH)_{1.6}\cdot H_2O$ and (b) $AlF_{1.7}(OH)_{1.3}\cdot H_2O$; na: 15000, (c) $AlF_{1.9}(OH)_{1.1}\cdot H_2O$; na:5400, (d) $AlF_x(O^iPr)_{3-x}\cdot{}^i$PrOH; na:15000, (e) $AlF_x(OEt)_{3-x}\cdot$MeOH; na: 12000.

Fig. 6 shows the corresponding ^{19}F MAS NMR spectra. For *a*–*c* only broad signals are observable with slight asymmetries. The maxima experience a high field shift with higher fluorine content, as more fluorine is incorporated into the structure: they can be found at about $\delta_{cs} = -146$ ppm for sample *a*, $\delta_{cs} = -150$ ppm for sample *b* and $\delta_{cs} = -154$ ppm for sample *c*, all in a typical region for bridging F-sites in octahedral AlF_xO_{6-x}-species, as earlier stated. Since sample *b* consists of more than one hydroxy fluoride phase a more complex spectrum could be expectable, but the experimental resolution used here, does not allow it to be resolved.

In contrast, the ^{19}F MAS NMR spectra of the amorphous aluminium alkoxide fluoride xerogels exhibit more diversity. For *d* we found a main signal at $\delta_{cs} = -162$ ppm and two smaller peaks at $\delta_{cs} = -154$ ppm and about $\delta_{cs} = -171$ ppm. On the other hand, the spectrum of the ethoxide/methanol xerogel is defined by one broad peak with its maximum at $\delta_{cs} = -163$ ppm and very broad "feet" at about $\delta_{cs} = -150$ ppm and $\delta_{cs} = -185$ ppm. Again, all the signals lay within the typical shift range for octahedral μ-F in AlF_xO_{6-x}-species. Only the most high-field shifted signals of the xerogels (and especially the signal at $\delta_{cs} = -185$ ppm) may also be contributions of terminal F-sites existent in the sol–gel derived xerogels. Table 3 lists the ^{19}F NMR parameters of the particular compounds as obtained by simulation, including three possibilities for the reproduction of the ^{19}F spectrum of *b*. These all lead to nearly the same average coordination, although the certain contributions differ. Interestingly, most of the line widths (FWHM about 5.0–6.0 kHz) correspond to those earlier stated for the aluminium fluoride hydrates (obtained on the same spectrometer

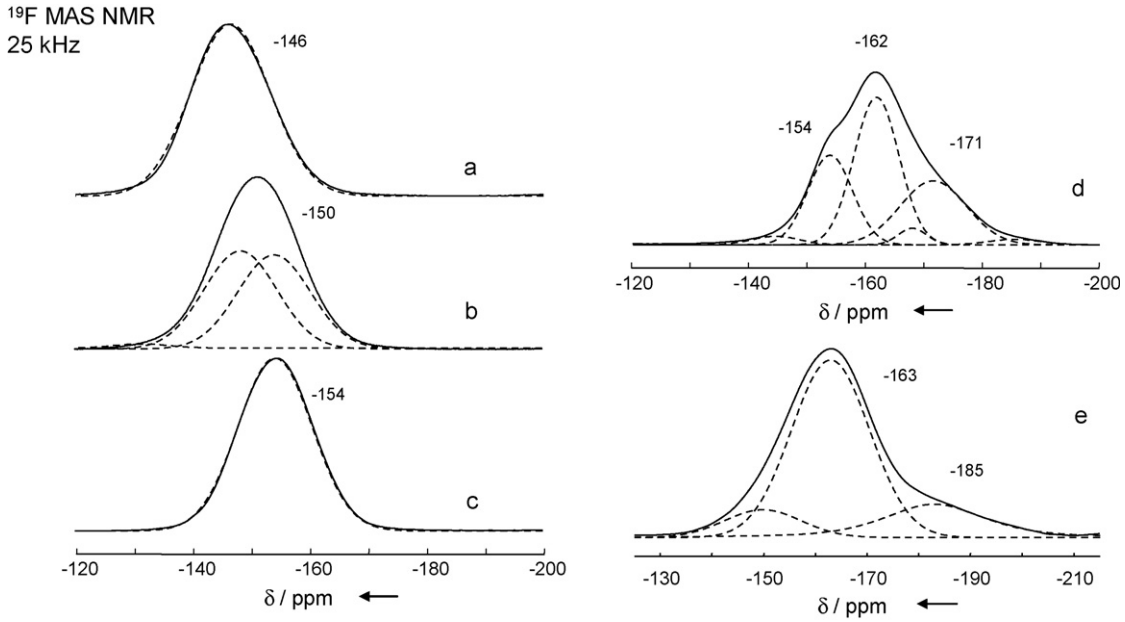

Fig. 6. ^{19}F MAS NMR spectra (—) of the hydroxy fluorides (*a*, *b*, *c*) and the alkoxide fluorides (*d*, *e*) at a spinning frequency of 25 kHz applying the *depth*-sequence. A possible deconvolution is shown with dashed lines (- - -) (number of accumulations: na): (a) $AlF_{1.4}(OH)_{1.6}\cdot H_2O$ and (b) $AlF_{1.7}(OH)_{1.3}\cdot H_2O$; na: 192, (c) $AlF_{1.9}(OH)_{1.1}\cdot H_2O$; na:16, (d) $AlF_x(O^iPr)_{3-x}\cdot{}^i$PrOH; na:192, (e) $AlF_x(OEt)_{3-x}\cdot$MeOH; na: 64.

Table 3
^{19}F NMR parameters as obtained by simulation of the particular spectra

Sample		δ_{CS} ^{19}F (ppm)	FWHM (kHz)	G/L[a]	Amount (%)	Possible assignment for AlF_xO_{6-x}[b]
a		−146.5	6.0	1	100	AlF_3O_3
b[c]	Model *I*	−151.2	6.1	1	100	Average: ≈$AlF_{3.4}O_{2.6}$
	Model *II*	−147.8	5.5	1	50	AlF_3O_3
		−154.2	5.5	1	50	AlF_4O_2
	Model *III*	−134.2	3.7	1	3	$AlFO_5$
		−144.7	3.9	1	16	AlF_2O_4
		−152.7	5.4	1	81	AlF_4O_2
c		−154.3	5.6	1	100	AlF_4O_2
d[d]		−153.9	3.4	1	25	AlF_4O_2
		−161.8	3.4	1	41	AlF_5O
		−171.5	5.0	1	26	t-F: AlF_4O_2 (?)
e		−149.9	6.6	1	11	Average: ≈AlF_5O
		−162.9	6.7	1	69	
		−183.0	8.6	0.5	20	
f[e]		−155.3	–	–	–	AlF_4O_2
g[e]		−161.8	–	–	–	AlF_5O_1

[a] G/L: *x* Gaussian/(1−*x*) Lorentzian.
[b] According to Fig. 7. Shown are the main contributions of species with the average AlF_xO_{6-x}-coordination.
[c] Model: possible decompositions of the single ^{19}F-central line.
[d] Three more contributions with an amount less or equal to 3% are present: δ_{CS} = −144.0, −168.0 and −185.5 ppm.
[e] Chemical shift of the signal maximum as observed in the appropriate spectra.

at the same MAS-frequency: α-AlF_3·3 H_2O: 5.9 kHz, nonahydrate: 5.0 kHz) [47].

3. Discussion

From the X-ray powder diffractograms (see Fig. 2 and supporting information Figure S1) it is obvious that the hydroxy fluoride phases are crystalline and therefore suitable here as model compounds. All Al-atoms are octahedrally coordinated in a mixed F/OH environment, resulting in a corner shared structure. So every F/OH-atom counts for one half to one Al-atom. The Al–F ratio (as, e.g. obtained from the elemental analysis) should reflect the average AlF_xO_{6-x}-coordination; for example, for an $AlF_x(OH)_{3-x}$-pyrochlore sample with the composition $AlF_2(OH)$ the average coordination would be $AlF_{4/2}(OH)_{2/2}$ (in Niggli description) or shorter, for simplification AlF_4O_2. However, the decomposition of the average AlF_xO_{6-x}-coordination into single contributing species implies more than one possibility (see, e.g. Table 3). Additionally, even more implications arise for attribution, if more than one phase is present (sample *b*).

As shown from ^{1}H MAS NMR, a discrimination between water (signal at about 4 ppm) and the bridging hydroxy groups (at 7.5 ppm) is derivable, but the differences are not well accentuated. For the alkoxide fluorides, the solvents involved lead to the main contributions of the observed spectra. For all of them the formation of a hydrogen bridged network can be stated.

The ^{27}Al MAS NMR spectra show a broad signal and an asymmetric upfield-decay for each sample. Both characteristics are mainly caused by distribution-effects: the superimposition and distribution of more than one certain AlF_xO_{6-x}-species and a distribution of bond lengths and angles. Different connection modes of the involved AlF_xO_{6-x}-octahedra (isolated, chains, planes or 3d-network) may also lead to several distinguishable species in the matrix and so to different smaller deviations in the certain spectra, as, for example, recently shown by Body for certain complex aluminium fluorides [48]. As all the maxima of the compounds lie within the range from 0 to −20 ppm, the conclusion is, that the main coordination is octahedral and is a mixed (hydr~/alk~)oxidic and fluoridic one: AlF_xO_{6-x} (*x* = 2–5). More information is not deducible at this point from the ^{27}Al MAS NMR spectra taken at 9.4 T as presented here.

Regardless, the main conclusions can be gathered by studying the ^{19}F MAS NMR spectra. Compiling the chemical shift values of the observed maxima in the ^{19}F MAS NMR spectra of the three crystalline hydroxy fluorides (*a*, *b*, and *c*) against the average AlF_xO_{6-x}-coordination, which is deduced from the data of the elemental analysis (s. also Table 3), a linear trend instantly becomes obvious (s. Fig. 7). For F in α- or β-AlF_3 (both consist of corner shared AlF_6-octahedra) the known chemical shift is δ_{CS} = −172 ppm (FWHM ≈ 3 kHz). A linear regression also taking into account the point just mentioned leads to the trend shown in

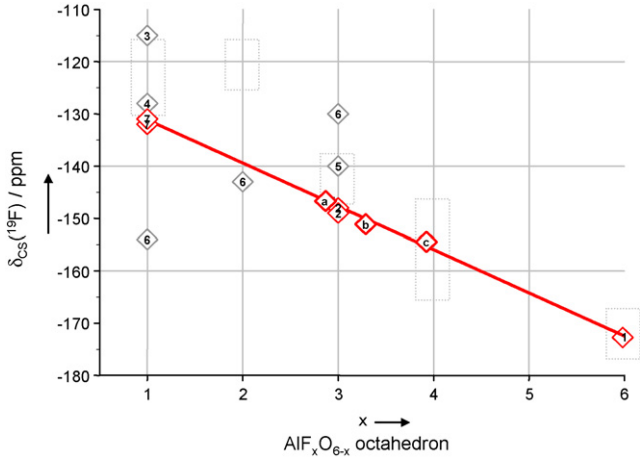

Fig. 7. ^{19}F Chemical shift trend analysis for AlF_xO_{6-x}-containing solids. In red: data obtained for the hydroxy fluorides *a*, *b* and *c*; and reported data for compounds which only contain Al, F, O and H in the matrix. For the linear regression the ^{19}F chemical shift of α-AlF_3 and β-AlF_3 was used as additional point. ◇ (*a*, *b*, *c*)—crystalline hydroxy fluorides (see also Table 3); ◇ (1)—α-AlF_3, β-AlF_3; ◇ (2)—*Kemnitz:* α-AlF_3·3 H_2O and AlF_3·9 H_2O [47]; ◇ (3)—*Taulelle:* $AlPO_4$-CJ2 aluminophosphate [50]; ◇ (4)—*Dumas:* $K[Al_2F(H_2O)_4(PO_4)_2]$ [52]; ◇ (5)—*Simon:* MIL-12 aluminophosphate [51]; ◇ (6)—*Fischer:* Fluorination of γ-Al_2O_3 [53]; ◇ (7)—*Allouche*: Fluorination of Al_{13} Kε-J (Keggin-structure) [49]. Grey boxes mark the diagram compiled by Chupas [46]. (For interpretation of the references to colour in this figure legend, the reader is referred to the web version of the article.)

Fig. 7 (R^2 = 0.994). An error for the AlF_xO_{6-x}-coordination of about 5% was estimated, bearing in mind the difficulties for determination of the exact F-content in such samples. The absolute error for the determination of the chemical shifts should be not larger than ±0.5 ppm.

Additionally, earlier reported data were incorporated (these data were not part of the linear regression). Surprisingly, in the cases of the aluminium fluoride hydrates [47] (see Fig. 7, no. 2) and of the fluorinated Al_{13}-Keggin [49] (Fig. 7, no. 7) the regression-straight is matched exactly. Interestingly the signals of the fluorine-atoms of α-AlF_3·3 H_2O and of the nonahydrate are at the "position" at $\delta_{CS} \approx -149$ ppm for a mean AlF_3O_3-coordination although all F-sites are in terminal position and so a more high field shifted position in the area of $\delta_{CS} \approx -173$ ppm would be expected. These findings can only be explained by the incorporation of the F-sites into a strong hydrogen bridged network [47].

For comparison the graph compiled by Chupas is also included in Fig. 7 (marked as boxes) [46]. For the crystalline phosphate and fluoride containing substances a downfield shift of the corresponding signals is obvious, because the components of the solids (and therefore the chemical surrounding) are slightly different in comparison to non-phosphate bearing substances [50–52]. The reported ^{19}F MAS NMR shifts of Fischer (Fig. 7, no. 6) are clear in opposition to the observed trend [53]. Fischer also identified different fluorine sites at the surface of fluorinated γ-Al_2O_3 and discussed the formation of AlF_3O_3, AlF_2O_4 and AlF_1O_5-species. The reported ^{19}F NMR shifts with respect to C_6F_6 were 9 ppm (−154 ppm) for $AlFO_5$, 20 ppm (−143 ppm) for AlF_2O_4 and 33 ppm (−130 ppm) for AlF_3O_3 [1] [53]. But as the fluorination mainly takes place at the surface of the alumina, the formation of terminal F-sites cannot be excluded.

Xu investigated NH_4F treated [Al]MCM-41-zeolites and assigned a signal at −155 ppm (^{27}Al: 0 ppm) to $AlFO_5$, which is the remaining species of the dealumination process; F should be mainly in terminal position [54].

Besides, some publications exist using nuclear magnetic resonance as analytical tool concerning AlF_xO_y-species in solution [55–57], in zeolites (dealumination process or fluorination) or other F containing solids on $AlPO_4$/SAPO basis [9,27,58–63]. But in the most cases no distinct assignment to certain species was set, which is in the case for amorphous compounds due to the observation of broad and/or overlapping signals.

As described at the beginning the average AlF_xO_{6-x}-coordination is reflected by the elemental analysis data and also by the appropriate ^{19}F MAS NMR spectra. The compiled graph (Fig. 7) should be a helpful tool for the interpretation of ^{19}F MAS NMR spectra, as it describes clearly for the first time the strong "linear" dependence of the "mean" ^{19}F chemical shift on the coordination of the single species. Following that, firstly a more precise interpretation of ^{19}F MAS NMR spectra was possible and secondly as shown later on, a prediction of the average chemical composition of related compounds can be made by solid-state NMR.

As an example sample *b* will now be discussed: three possible decompositions are shown in Table 3 (marked as models *I*, *II* and *III*). The maximum of the observed peak is at δ_{CS} = −150 ppm; the composition is given with $AlF_{1.7}(OH)_{1.3}$·H_2O, which means an average coordination from $AlF_{3.4}O_{2.6}$ (model *I*).

In a second approximation, one possible explanation may be the superimposition of the main signals by two species as shown in the spectra Fig. 6b: one with a chemical shift at $\delta_{CS} \approx -148$ ppm, assignable to AlF_3O_3 (see Fig. 7) and an equal contribution from an AlF_4O_2-species at $\delta_{CS} \approx -154$ ppm (see Fig. 7). Since ^{19}F has a spin of $I = 1/2$ the integrals of the deconvoluted signals represent different species. A molar ratio of Al:F like 1:1.7 (average coordination $AlF_{3.4}O_{2.6}$) would be plausible by the summation of about 50% AlF_4O_2-octahedra and 50% AlF_3O_3-octahedra (Table 3, model *II*) in the crystal structure, as it is also suggested by XRD, since two phases were observed ("$AlF_2(OH)$" and "$AlF_{1.5}(OH)_{1.5}$"). Regardless, the involved species may be distributed in a third way: the amount of the AlF_4O_2-units in the structures may be much higher. Then to reach the average coordination, the assumption of small contributions from AlF_2O_4- or $AlFO_5$-octahedra is necessary (e.g. as nearly reflected by model *III*, Table 3). Although model *II* and *III* may reflect possible meaningful (de)compositions, they are at least models and first approximations. In "solid-state reality" however, broader distributions of species as well as bond geometries may play a role.

Simultaneously this clearly shows the risk for misinterpretation of such spectra since similar considerations would also hold for samples *a* and *c*. The question of the exact composition might be resolved by the application of ^{27}Al MAS NMR techniques in correlation with the data presented here. In spite of that, the model for the interpretation of ^{19}F MAS NMR spectra derived here can be used for the prediction of the average AlF_xO_{6-x}-coordination in amorphous aluminium alkoxide fluorides or aluminium (hydr)oxide fluorides as discussed in the following.

For the aluminium isopropoxide fluoride (Fig. 6, sample *d*) at least two species are assignable. At δ_{CS} = −162 ppm AlF_5O-species and at δ_{CS} = −154 ppm AlF_4O_2 were to be expected (see Fig. 7). For the third signal two explanations have to be considered; either a certain amount of AlF_6 or possible terminal sites may be accountable for the signal around δ_{CS} = −172 ppm. An average coordination between AlF_4O_2 and AlF_5O is expected. For an analogous batch a chemical composition of $AlF_{2.3}(O^iPr)_{0.7}$·z^iPrOH was determined [23]. Both the elemental analysis as well as the appropriate ^{19}F MAS NMR and ^{27}Al MAS NMR spectra of these two isopropoxide fluoride batches only differ little. The analogy and accordance with the proposed model (^{19}F chemical shift trend analysis) is obvious. The ethoxide/methanol xerogel shows several contributions which are relatively broad and hardly to distinguish. The main peak arises at δ_{CS} = −163 ppm, assignable to an average AlF_xO_{6-x} distribution with its maximum at AlF_5O. Since more fluorine is incorporated in the structure, a derived composition of $AlF_{2.5}(OEt)_{0.5}$·zMeOH and higher is expected.

The samples *f* and *g* (see Table 1, 3) represent two amorphous aluminium hydroxy fluorides chosen as examples. The corresponding NMR data are given in Table 3. These were prepared here in quite a similar way using dried THF as solvent and aqueous HF as fluorinating agent for another area of interest [64]. However, as these compounds are of course related to the study here, the chemical shift trend analysis may be used for the prediction of local structures. Samples *f* and *g* exhibit a rising F-content (from *f* to *g*) and for *f* and *g* the model can be used here because the Al-atoms are in a mixed O/F environment and octahedrally coordinated. The observed ^{19}F chemical shift of the maximum for sample *f* is found at $\delta_{CS} \approx -155.3$ ppm, so an average coordination of AlF_4O_2 is expected (see Fig. 7) (elemental analysis of the same sample dried at 180 °C gave the composition: n_{Al}:n_F 1:2, "AlF_2OH"≡AlF_4O_2-octahedron). Similar considerations hold for sample *g*: as the maximum of the ^{19}F-signal is found at $\delta_{CS} \approx -161.8$ ppm, an average coordination AlF_5O can be assumed for this compound (elemental analysis of the same sample dried at 180 °C gave the empirical formula "AlF_3·$0.5H_2O$", which is equal to a F–O ratio from 5.14 to 0.86). Both attributions are only conclusive if the incorporated F is mainly in corners sharing positions of the involved AlF_xO_{6-x}-octahedra, but the argumentation for these

[1] The reference itself was given with a chemical shift δ = −163 ppm for C_6F_6 against $CFCl_3$. Chemical shifts in parentheses are stated with respect to $CFCl_3$ (0 ppm).

samples is underlined by the appropriate ^{27}Al NMR data. The ^{27}Al NMR signals of both compounds lie in the typical region for octahedrally coordinated Al, and a high field shift of the maximum of the observed ^{27}Al MAS NMR signals from $\delta_{CS} \approx -6$ ppm for *f*– $\delta_{CS} \approx -12$ ppm for *g* (spectra not shown), clearly confirms the model proposed here. For AlF_5O (*g*) a more negative ^{27}Al NMR shift would be expected in comparison to AlF_4O_2 [64].

4. Conclusions

The preparation of wet aluminium alkoxide fluoride gels with a subsequent evaporation of the solvent and hydrolysis at ambient conditions leads to crystalline aluminium hydroxy fluorides with tunable Al:F ratios for certain molar ratios (Al:F 1:3, 1:2, solvent ^{i}PrOH). Since the structure only consists of corner shared AlF_xO_{6-x}-octahedra, different average AlF_xO_{6-x}-coordinations dependent on the molar Al:F ratio, are expected. Furthermore, as shown in Fig. 7, a clear relationship between the physico-chemical property ^{19}F "chemical shift" and the average coordination can be deduced; for other properties, e.g. binding energies derived from XPS/XAES-spectroscopy similar results can be expected. Sol–gel derived aluminium alkoxide fluorides, as intermediates to HS-AlF_3, are X-ray amorphous – no structural information can be gained from that. Nevertheless, a strong structural relationship between the crystalline hydroxy fluorides and the amorphous alkoxide fluorides was demonstrated.

These relationships do not hold for ^{1}H MAS NMR, as the main contributions in the particular spectra are solvent dominated. For ^{27}Al MAS NMR and as shown especially for ^{19}F MAS NMR strong similarities are obvious.

The strong correlation between ^{19}F chemical shift and the average composition of AlF_xO_{6-x}-species allows us to develop a chemical shift trend analysis for solid-state NMR. Due to the strong correlation, a satisfying match of the discovered trend is observed for samples containing exclusively Al, F, O and H in the matrix. ^{19}F-signals of fluorine containing aluminium phosphates as previously published are downfield shifted in relation to the straight presented here [46]. The main requirements of the compounds to match the straight presented in Fig. 7 are: octahedral AlF_xO_y-species as building units, linked over their corners and possibly the incorporation into a hydrogen bridge-bond network.

The transfer of the ^{19}F chemical shift trend analysis to related compounds, for example, hydrated amorphous aluminium hydroxy fluorides and aluminium alkoxide fluorides (with residual solvent) is possible. It now allows a more distinct interpretation of the appropriate spectra and the prediction of the average chemical surrounding of the Al-atoms.

For this reason a prediction of the elemental composition $AlF_x(OX)_{3-x}$ made by solid-state NMR becomes possible.

Finally, the shown correlation opens an avenue for a more precise interpretation and decomposition of experimental ^{19}F MAS NMR spectra of crystalline and amorphous AlF_xO_y containing solids.

5. Experimental

5.1. Sample preparation

All chemicals were used as delivered.

Samples *a* and *b* were synthesised with a variation of the methods described in [19,23]. The resulting wet aluminium alkoxide–fluoride gels (molar ratios n[Al(O^{i}Pr)$_3$]:n[HF] for *a* 1:2, for *b* 1:3) were transferred into an evaporating dish and exposed to air. After few days white xerogels/solids were formed after evaporation of the incorporated alcohol and hydrolysis of remaining alkoxide groups, which could be characterised as hydrated forms of crystalline aluminium hydroxy fluorides $AlF_x(OH)_{3-x}\cdot zH_2O$ in pyrochlore structure ($z \approx 1$).

Sample *c* was prepared according to the method described by Menz [30]: basic aluminium acetate (Al(OH)ac$_2$) was suspended in distilled water and heated after the addition of aqueous HF (molar ratio Al:F 1:2). The precipitate was filtrated and washed with hot H_2O and afterwards dried under access of air at ambient conditions. The bright white powdered solid was also identified as pyrochlore-$AlF_x(OH)_y\cdot zH_2O$ ($z \approx 1$).

Samples *d* and *e* were prepared as mentioned in [22] using Schlenk-techniques by sol–gel reaction of an aluminium alkoxide with anhydrous alcoholic HF (n[Al(OR)$_3$]:n[HF] = 1:3). Drying in vacuum leads to X-ray amorphous aluminium alkoxide fluoride–xerogels, which were stored in a glove-box.

Samples *f* and *g* (amorphous $AlF_x(OH)_{3-x}\cdot zH_2O$) were prepared in a similar way using dried THF as solvent and aqueous HF (molar ratios 1:2 and 1:3). The resulting gels were dried in vacuum at 70 °C and handled afterwards in air. Further details are described elsewhere [64].

5.2. Elemental analysis and XRD-measurements

The elemental analysis of the samples was performed with a LECO CHNS-932 combustion equipment (C, H, N). The fluoride contents were determined with a fluoride sensitive electrode after conversion of the solids with Na_2CO_3/K_2CO_3 into a soluble form. The aluminium contents of the hydroxy fluorides were determined with ICP OES method (IRIS Intrepid HR DUO) after a microwave assisted (ETHOS plus) conversion with a H_3PO_4/HNO_3 – mixture into a soluble form.

The presented X-ray diffractograms were measured on a Seifert XRD3003TT diffractometer with Cu Kα radiation.

5.3. Solid-state NMR

^{19}F,^{27}Al, and ^{1}H MAS NMR spectra were recorded on a Bruker AVANCE 400 spectrometer (Larmor frequencies: $\nu_{19_F} = 376.4$ MHz; $\nu_{27_{Al}} = 104.3$ MHz, $\nu_{1_H} = 400.1$ MHz) using a 2.5 mm MAS probe (Bruker Biospin).

^{19}F MAS NMR ($I = 1/2$) spectra were recorded with a $\pi/2$ pulse duration of p1 = 2.0 μs, a spectrum width of 400 kHz, and a recycle delay of 3 s for the xerogels. Spectral changes for longer recycle delays were checked. The isotropic chemical shifts δ_{CS} of ^{19}F resonances are given in respect to the $CFCl_3$ standard. Existing background signals of ^{19}F and ^{1}H could be completely suppressed with the application of a phase-cycled depth pulse sequence according to Cory and Ritchey [65]. ^{19}F spectra were simulated using dmfit2007 [66].

^{27}Al MAS NMR ($I = 5/2$) spectra were recorded with an excitation pulse duration of 1 μs. The chemical shifts of ^{27}Al are given with respect to $AlCl_3$ in aqueous solution (0 ppm). The recycle delay was chosen as 1 s.

^{1}H MAS studies were made with a $\pi/2$ pulse length of 2.2 μs and a recycle delay of 3 s for the alkoxide fluorides and up to 10 s for the hydroxy fluorides and a spectrum width from 100 to 300 kHz. The characteristics of the observed signals were checked for longer recycle delays. Values of the isotropic chemical shifts of ^{1}H are given with respect to TMS.

The accumulation numbers for each spectrum are given with the particular spectra.

Acknowledgements

The Deutsche Forschungsgemeinschaft is kindly acknowledged for financial support with the project Ke 489/29-1. The EU is

acknowledged for support of part of this work through the 6th Framework Programme (FUNFLUOS, Contract No. NMP3-CT-2004-5005575).

Dr. D. Heidemann is acknowledged for fruitful discussions, Dr. A. Zehl, U. Kätel for the elemental analysis and S. Bäßler for the F-determination and especially for performing the thermogravimetric measurements. Ellen Keller and Dirk Sewohl are noticed for preparation of some hydroxy fluorides.

Furthermore DC C. Stosiek and DC I. Buchem are kindly acknowledged for providing the data of the respective samples.

Appendix A. Supplementary data

Supplementary data associated with this article can be found, in the online version, at doi:10.1016/j.jfluchem.2008.04.015.

References

[1] L. Zhang, H. Eckert, Solid State Nucl. Mag. Reson. 26 (2004) 132–146.
[2] R. Corriu, D. Leclercq, Angew. Chem. 108 (1996) 1524–1540.
[3] D.C. Bradley, Chem. Rev. 89 (1989) 1317–1322.
[4] Z. Lu, E. Lindner, H.A. Mayer, Chem. Rev. 102 (2002) 3543–3578.
[5] B.L. Cushing, V.L. Kolesnichenko, C.J. O'Connor, Chem. Rev. 104 (2004) 3893–3946.
[6] D. Boyer, R. Mahiou, Chem. Mater. 16 (2004) 2518–2521.
[7] J.-B. Choi, J.-S. Rho, J. Korean Ind. Eng. Chem. 11 (2000) 969–973.
[8] S. Lepoutre, D. Boyer, R. Mahiou, Opt. Mater. 28 (2006) 592–596.
[9] L. Zhang, C.C. de Araujo, H. Eckert, Chem. Mater. 17 (2005) 3101–3107.
[10] E. Kemnitz, U. Groß, S. Rüdiger, C.S. Shekar, Angew. Chem. Int. Ed. 42 (2003) 4251–4254.
[11] S. Rüdiger, U. Groß, E. Kemnitz, J. Fluorine Chem. 128 (2007) 353–368.
[12] M. Ahrens, K. Schuschke, S. Redmer, E. Kemnitz, Solid State Sci. 9 (2007) 833–837.
[13] U. Groß, S. Rüdiger, E. Kemnitz, Solid State Sci. 9 (2007) 838–842.
[14] S. Wuttke, G. Scholz, S. Rüdiger, E. Kemnitz, J. Mater. Chem. 17 (2007) 4980–4988.
[15] H. Krüger, E. Kemnitz, A. Hertwig, U. Beck, Presented at 4th International Conference on Spectroscopic Ellipsometry, Stockholm, Sweden, June, 2007.
[16] K. Scheurell, E. Kemnitz, J. Mater. Chem. 15 (2005) 4845–4853.
[17] K. Scheurell, G. Scholz, E. Kemnitz, J. Solid State Chem. 180 (2007) 749–758.
[18] P.T. Patil, A. Dimitrov, H. Kirmse, W. Neumann, E. Kemnitz, Appl. Catal. B 78 (2008) 80–91.
[19] S. Rüdiger, G. Eltanany, U. Groß, E. Kemnitz, J. Sol–Gel Sci. Technol. 41 (2007) 299–311.
[20] T. Krahl, E. Kemnitz, J. Fluorine Chem. 127 (2006) 663–678.
[21] U. Groß, S. Rüdiger, E. Kemnitz, K.W. Brzezinka, S. Mukhopadhyay, C. Bailey, A. Wander, N. Harrison, J. Phys. Chem. A 111 (2007) 5813–5819.
[22] R. König, G. Scholz, N.H. Thong, E. Kemnitz, Chem. Mater. 19 (2007) 2229–2237.
[23] R. König, G. Scholz, E. Kemnitz, Solid State Nucl. Mag. Reson. 32 (2007) 78–88.
[24] J. Kramer, K.R. Koch, Inorg. Chem. 46 (2007) 7466–7476.
[25] V. Lacassagne, C. Bessada, P. Florian, S. Bouvet, B. Ollivier, J.P. Coutures, D. Massiot, J. Phys. Chem. B 106 (2002) 1862–1868.
[26] C.D. Wagner, L.H. Gale, R.H. Raymond, Anal. Chem. 51 (1979) 466–482.
[27] R.B. Borade, A. Clearfield, J. Chem. Soc. Faraday T 91 (1995) 539–547.
[28] J.M. Cowley, T.R. Scott, J. Am. Chem. Soc. 70 (1948) 105–109.
[29] J.L. Fourquet, M. Riviere, A. Le Bail, Eur. J. Solid State Inorg. Chem. 25 (1988) 535–540.
[30] D.H. Menz, C. Mensing, W. Hönle, H.G. von Schnering, Z. Anorg. Allg. Chem. 611 (1992) 107–113.
[31] A. Hess, E. Kemnitz, A. Lippitz, W.E.S. Unger, D.H. Menz, J. Catal. 148 (1994) 270–280.
[32] M. Grobelny, J. Fluorine Chem. 10 (1977) 63–73.
[33] A. Demourgues, L. Francke, E. Durand, A. Tressaud, J. Fluorine Chem. 114 (2002) 229–236.
[34] L. Francke, E. Durand, A. Demourgues, A. Vimont, M. Daturi, A. Tressaud, J. Mater. Chem. 13 (2003) 2330–2340.
[35] P.E. Rosenberg, Canad. Mineral. 44 (2006) 125–134.
[36] G.A. Desborough, O. Rostad, Am. Mineral. 65 (1980) 1057–1058.
[37] O.V. Bulgakov, T.V. Antipina, Zh. Fiz. Khim. 42 (1967) 2060–2062.
[38] A.S. Korobitsyn, G.N. Sharapova, O.V. Katorina, I.A. Leonteva, L.N. Kalitina, T.A. Ustyantseva, Z.I. Shishkina, Zh. Prikl. Khim. 53 (1980) 2350–2353.
[39] G.A. Kirakosyan, L.N. Komissarova, L.A. Nesterova, G.Y. Pushkina, V.F. Chuvaev, V.M. Shatskii, Zh. Neorg. Khim. 22 (1977) 1460–1464.
[40] D. Dambournet, A. Demourgues, C. Martineau, S. Pechev, J. Lhoste, J. Majimel, A. Vimont, J.-C. Lavalley, C. Legein, J.Y. Buzaré, F. Fayon, A. Tressaud, Chem. Mater. 20 (2008) 1459–1469.
[41] D. Dambournet, A. Demourgues, C. Martineau, E. Durand, J. Majimel, A. Vimont, H. Leclerc, J.-C. Lavalley, M. Daturi, C. Legein, J.Y. Buzaré, F. Fayon, A. Tressaud, J. Mater. Chem. (2008), doi:10.1039/b718856k.
[42] N. Herron, D.L. Thorn, R.L. Harlow, G.A. Jones, J.B. Parise, J.A. Fernandezbaca, T. Vogt, Chem. Mater. 7 (1995) 75–83.
[43] S. Rüdiger, U. Groß, M. Feist, H.A. Prescott, C.S. Shekar, S.I. Troyanov, E. Kemnitz, J. Mater. Chem. 15 (2005) 588–597.
[44] R.L. Johnson, B. Siegel, Nature 210 (1966) 1256–1257.
[45] J. Rodriguez-Carvajal, FULLPROF version January 2006, ILL (unpublished).
[46] P.J. Chupas, D.R. Corbin, V.N.M. Rao, J.C. Hanson, C.P. Grey, J. Phys. Chem. B 107 (2003) 8327–8336.
[47] E. Kemnitz, U. Groß, S. Rüdiger, G. Scholz, D. Heidemann, S.I. Troyanov, I.V. Morosov, M.H. Lemee-Cailleau, Solid State Sci. 8 (2006) 1443–1452.
[48] M. Body, C. Legein, J.-Y. Buzaré, G. Silly, Eur. J. Inorg. Chem. 14 (2007) 1980–1988.
[49] L. Allouche, F. Taulelle, Chem. Commun. 16 (2003) 2084–2085.
[50] F. Taulelle, M. Pruski, J.P. Amoureux, D. Lang, A. Bailly, C. Huguenard, M. Haouas, C. Gerardin, T. Loiseau, G. Ferey, J. Am. Chem. Soc. 121 (1999) 12148–12153.
[51] N. Simon, N. Guillou, T. Loiseau, F. Taulelle, G. Ferey, J. Solid State Chem. 147 (1999) 92–98.
[52] E. Dumas, F. Taulelle, G. Ferey, Solid State Sci. 3 (2001) 613–621.
[53] L. Fischer, V. Harle, S. Kasztelan, J.B.D. de la Caillerie, Solid State Nucl. Mag. Reson. 16 (2000) 85–91.
[54] M.C. Xu, W. Wang, M. Seiler, A. Buchholz, M. Hunger, J. Phys. Chem. B 106 (2002) 3202–3208.
[55] N.A. Matwiyoff, W.E. Wageman, Inorg. Chem. 9 (1970) 1031–1036.
[56] S.K. Sur, R.G. Bryant, Zeolites 16 (1996) 118–124.
[57] O.B. Vistad, E.W. Hansen, D.E. Akporiaye, K.P. Lillerud, J. Phys. Chem. A 103 (1999) 2540–2552.
[58] M. Pruski, D.P. Lang, C. Fernandez, J.P. Amoureux, Solid State Nucl. Mag. Reson. 7 (1997) 327–331.
[59] C.P. Grey, D.R. Corbin, J. Phys. Chem. 99 (1995) 16821–16823.
[60] H.M. Kao, P.C. Chang, J. Phys. Chem. B 110 (2006) 19104–19107.
[61] P.J. Chupas, C.P. Grey, J. Catal. 224 (2004) 69–79.
[62] P.J. Chupas, M.F. Ciraolo, J.C. Hanson, C.P. Grey, J. Am. Chem. Soc. 123 (2001) 1694–1702.
[63] E. Decanio, J.W. Bruno, V.P. Nero, J.C. Edwards, J. Catal. 140 (1993) 84–102.
[64] C. Stosiek, G. Scholz, E. Kemnitz, Chem. Mater., submitted for publication.
[65] D.G. Cory, W.M. Ritchey, J. Magn. Reson. 80 (1988) 128–132.
[66] D. Massiot, F. Fayon, M. Capron, I. King, S. Le Calve, B. Alonso, J.O. Durand, B. Bujoli, Z.H. Gan, G. Hoatson, Magn. Reson. Chem. 40 (2002) 70–76.